Tree Physiology Advance Access published June 9, 2015

Tree Physiology 00, 1–12
doi:10.1093/treephys/tpv040

Research paper

Patterns of drought-induced embolism formation and spread in living walnut saplings visualized using X-ray microtomography

Thorsten Knipfer[1], Craig R. Brodersen[2], Amr Zedan[1], Daniel A. Kluepfel[3] and Andrew J. McElrone[1,3,4]

[1]Department of Viticulture and Enology, University of California, Davis, CA 95616, USA; [2]School of Forestry and Environmental Studies, Yale University, 195 Prospect Street, New Haven, CT 06511, USA; [3]US Department of Agriculture, Agricultural Research Service, Davis, CA 95616, USA; [4]Corresponding author (ajmcelrone@ucdavis.edu)

Received November 4, 2014; accepted April 27, 2015; handling Editor Nathan Phillips

Embolism formation and spread are dependent on conduit structure and xylem network connectivity. Detailed spatial analysis has been limited due to a lack of non-destructive methods to visualize these processes in living plants. We used synchrotron X-ray computed tomography (microCT) to visualize these processes in vivo for *Juglans microcarpa* Berl. saplings subjected to drought, and also evaluated embolism repair capability after re-watering. Cavitation was not detected in vivo until stem water potentials (Ψ_{stem}) reached −2.2 MPa, and loss of stem hydraulic conductivity as derived from microCT images predicted that 50% of conductivity was lost at Ψ_{stem} of ~ −3.5 MPa; xylem vulnerability as determined with the centrifuge method was comparable only in the range of Ψ_{stem} from −2.5 to −3.5 MPa. MicroCT images showed that cavitation appeared initially in isolated vessels not connected to other air-filled conduits. Once embolized vessels were present, multiple vessels in close proximity cavitated, and 3-D analysis along the stem axis revealed some connections between cavitated vessels. A tomography-derived automated xylem network analysis found that only 36% of vessels had one or more connections to other vessels. Cavitation susceptibility was related to vessel diameter, with large diameter vessels (>40 μm, mean diameter 25–30 μm) cavitating mainly under moderate stress (Ψ_{stem} > −3 MPa) and small diameter vessels (<30 μm) under severe stress. After re-watering there was no evidence for short or longer term vessel refilling over 2 weeks despite a rapid recovery of plant water status. The low embolism susceptibility in 1-year-old *J. microcarpa* may aid sapling survival during establishment.

Keywords: air-seeding, cavitation, *Juglans microcarpa*, microCT, network connectivity, nucleation, water stress, xylem.

Introduction

Water is transported through plant xylem under tension (Dixon and Joly 1895, Tyree and Zimmermann 2002), and is considered metastable and vulnerable to cavitation when xylem tension exceeds a certain threshold (Tyree and Sperry 1989). Gas emboli that form in conduits after cavitation create blockages and reduce whole-plant hydraulic transport capacity. Extensive xylem embolism induced by severe drought can lead to plant death (Brodribb and Cochard 2009, Choat et al. 2012, Choat 2013). Embolism repair following re-watering is one mechanism to restore water transport capacity and prevent mortality (Brodersen et al. 2010, Knipfer et al. 2015).

When plants are subjected to drought stress, air can be sucked from an embolized vessel into the lumen of a water-filled vessel via inter-vessel connections (Zimmermann and Brown 1971, Pickard 1981, Tyree and Sperry 1989, Pockman et al. 1995, Tyree and Zimmermann 2002). Using synchrotron-based X-ray computed microtomography (microCT), this type of drought-induced embolism spread has been visualized recently and directly in both angiosperm and gymnosperm species (grapevine, Brodersen et al. 2013*a*; redwood, Choat et al. 2015). However, the spread of embolism by air-seeding requires the existence of at least one air-filled conduit that is present initially or could form by herbivory or other mechanical damage

(Tyree and Sperry 1989). For coastal redwood, Choat et al. (2015) showed that embolized conduits appear initially in isolation (i.e., no connection to adjacent air-filled conduits) and served as an important air source for embolism spread. The occurrence of conduits that cavitate in isolation suggests that mechanisms of nucleation other than air-seeding operate in xylem (Pickard 1981, Tyree and Sperry 1989). Additional work is needed to elucidate mechanisms involved in drought-induced embolism formation and spread in relation to xylem structure (e.g., vessel dimensions, network connectivity) across species.

Much recent debate has focused on the reliability of destructive hydraulic measurements to accurately assess vulnerability to cavitation and conduit functional status (Choat et al. 2010, Cochard et al. 2010, 2013, 2015, Jacobsen and Pratt 2012, McElrone et al. 2012, Sperry et al. 2012, Wheeler et al. 2013, Rockwell et al. 2014, Torres-Ruiz et al. 2014, Wang et al. 2014, Hacke et al. 2015). Consensus has not yet been reached and more work is needed to assess hydraulic methods and develop standard protocols. However, literature suggests that invasive hydraulic methods can dramatically overestimate xylem vulnerability (e.g., laurel, Cochard et al. 2015; olive, Torres-Ruiz et al. 2014). In grapevines, the xylem was found to be less susceptible to cavitation when analysed in vivo than previously reported using some invasive hydraulic methods (Choat et al. 2010, McElrone et al. 2012, Brodersen et al. 2013*a*). MicroCT has the advantage that xylem vulnerability can be determined in vivo (McElrone et al. 2013), and has been suggested as one reference technology to quantify xylem embolism and validate hydraulic measurements (Cochard et al. 2015, Rosner 2015). Here we use microCT to track patterns of embolism formation and spread in walnut saplings, and compare results with the commonly used centrifuge technique to assess its reliability for rapid screening of large amounts of germplasm material.

Juglans microcarpa Berl. is distributed naturally from southwestern Kansas through Oklahoma to central New Mexico and Texas, and grows on dry, rocky hillsides and within the riparian forest (http://plants.usda.gov/java/). Accessions of this species from a large germplasm collection are being evaluated as potential rootstocks for commercial walnut production. In other *Juglans* species, xylem embolism is known to significantly reduce hydraulic transport capacity (Tyree et al. 1993, Ameglio et al. 2002). Understanding traits that contribute to drought resistance and recovery for this species and developing appropriate methods to assess them are needed to effectively and rapidly screen large germplasm collections. In this study of *J. microcarpa*, drought-induced embolism susceptibility and spatial patterns of embolism formation and spread were examined in vivo using microCT. Based on microCT data, the spatial arrangement of xylem vessels was visualized in 3-D and quantitative estimates of inter-vessel connectivity were obtained using a Tomography-derived Automated Network Analysis of Xylem (TANAX) software (Brodersen et al. 2011). Percentage loss of stem hydraulic conductivity (PLC) in response to drought was derived from microCT images, and compared with hydraulic measurements using the centrifuge method. Vessel diameter distribution profiles were generated to investigate whether embolism susceptibility was related to vessel diameter. To test for embolism repair in vivo, drought-stressed saplings were scanned multiple times after re-watering.

Materials and methods

Plant material

One-year-old saplings of *J. microcarpa* were grown from seed at the USDA-ARS Germplasm Repository in Davis, CA, USA. Saplings were ~40–60 cm in height growing in 0.5-l pots filled with soil (40% washed sand, 20% sphagnum peat moss, 20% redwood compost, 20% pumice rock). Saplings were maintained in well-watered condition in a greenhouse, and were drip irrigated twice daily with water supplemented with calcium (90 $\mu g\ ml^{-1}$), magnesium (24 $\mu g\ ml^{-1}$), potassium (124 $\mu g\ ml^{-1}$), nitrogen as NH_4^+ (6 $\mu g\ ml^{-1}$), nitrogen as NO_3^- (96 $\mu g\ ml^{-1}$), phosphorus (26 $\mu g\ ml^{-1}$), sulphur (16 $\mu g\ ml^{-1}$), iron (1.6 $\mu g\ ml^{-1}$), manganese (0.27 $\mu g\ ml^{-1}$), copper (0.16 $\mu g\ ml^{-1}$), zinc (0.12 $\mu g\ ml^{-1}$), boron (0.26 $\mu g\ ml^{-1}$) and molybdenum (0.016 $\mu g\ ml^{-1}$) at pH 5.5–6.0. To induce water stress by drought, irrigation was removed up to 3 days prior to scanning, and recovery was evaluated at various points after re-watering during the scanning sessions.

X-ray microtomography

Saplings ($n = 18$) were transported from the greenhouse facilities at the University of California in Davis to the X-ray microtomography facility (Beamline 8.3.2) at the Advanced Light Source (ALS) at Lawrence Berkley National Laboratory. Within 15 min of scanning, plant water status was determined by measuring stem water potential (Ψ_{stem}) using a Scholander Pressure Chamber (Plant Moisture Stress Model 600, PMS Instrument Company, Albany, OR, USA); Ψ_{stem} was measured on leaves that had been covered with a sealed and foiled plastic bag for more than 20 min. When drought stress was sufficient to induce a desired Ψ_{stem}, the pot was placed in an aluminium cage that was fixed on an air-bearing stage, and a plastic cylinder was mounted on top of the cage to reduce vibrations and stem movement during scanning (Brodersen et al. 2010, 2013*a*). The stem was scanned just above the soil at 15 keV in the synchrotron X-ray beam while the sapling was rotating in 0.25° increments yielding 1440 two-dimensional images with a ~4.5 µm pixel resolution on a 4008 × 2672 pixel CCD camera (#PCO 4000, Cooke Corporation, Kehlheim, Germany). The acquired longitudinal images were reconstructed into a 'stack' of multiple transverse. TIF images using Octopus 8.3 software (Institute for Nuclear Sciences, Ghent University, Belgium). 3-D reconstructions of embolized vessels were generated with Avizo 6.2. software (FEI Company, Hillsboro, OR, USA). An 'edge-preserving smoothing' filter was applied first to

enhance contrast between voxels of gas-filled vessels and surrounding tissue. Subsequently, embolized vessel lumina were selected manually using the 'Label-field' segmentation editor and then displayed using the 'SurfaceGen' volume rendering module. Most saplings used to evaluate embolism formation and spread ($n = 15$) were subjected to a single scan. Three additional saplings were scanned multiple times to track spatial and temporal dynamics of embolism during a dry-down. Following drought stress, a subset of saplings were also re-watered and subjected to multiple microCT scans for up to 2 weeks to evaluate refilling potential (i.e., embolism repair) and rehydration.

Image analysis for vessel number and diameter

For each of the saplings subjected to microCT scans, the number and diameter of embolized vessels were determined from a representative transverse microCT image using the 'Analyze Particle' tool in Fiji software (www.fiji.sc, ImageJ). Based on measurements of vessel area (A), vessel diameter (d) was derived according to $A = \pi (d/2)^2$. After microCT scans were completed, stem segments in the region of the scan were harvested and preserved in 70% ethanol. Stem segments were sectioned with a sliding microtome (American Optical Company, Buffalo, NY, USA), stained with 1% (aq.) toluidine blue O for 30 s before washing them with water and placed on a microscope slide. Light micrographs were acquired with a digital camera mounted on a microscope (#DFC425, Leica Microsystems Limited, Buffalo Grove, IL, USA). From light micrographs, total vessel numbers and corresponding diameters were determined using the 'Point selection' and 'Polygon selection' tool in Fiji software. The percentage of embolized vessels was calculated by [(number of embolized vessels/total number of vessels) × 100%]. Distribution profiles of vessel diameter were generated for size classes in diameter of 0–5, 5–10 μm, etc. Vessel frequency was determined by [(number of vessels per size class/total number of vessels) × 100%]. Vessel distribution profiles were first generated for saplings ($n = 9$) for which both light and microCT images of sufficient resolution were available, and subsequently vessel frequency per size class was averaged. This analysis was performed for the entire xylem region, and separately for the 'inner' (i.e., towards pith), 'middle' and 'outer' (i.e., towards cambium) xylem regions to determine radial patterns of embolism formation with increasing stress. The three xylem regions were separated as follows: a line was drawn using Fiji software from the inner to the outer xylem edge at positions 0°, 90°, 180° and 360°. Each of the four lines was divided into three equal length portions, and two ellipses were drawn that intersected all four lines either at the transition of inner-to-middle region or at middle-to-outer region.

Xylem network analysis

Using TANAX software (Brodersen et al. 2011), vessel connectivity was determined from transverse microCT images ($n = 1318$) of a 5.93-mm-long portion of a dried (at 40 °C for 48 h) stem segment of *J. microcarpa* (see Figure S1 available as Supplementary Data at *Tree Physiology* Online). Before analysis, microCT images were processed in Fiji software and Avizo (FEI Company) to reduce scan noise and to accurately identify vessel lumen. Subsequently, the entire stack of images was processed with the TANAX software, and vessel number and distance between lumina of vessels were determined (for details, see Brodersen et al. 2011). TANAX was programmed to establish an inter-vessel connection when the distance between neighbouring vessel lumina was within the 'threshhold-distance' <12 μm (i.e., estimated thickness of the double vessel wall of adjacent vessels as determined by light microscopy and higher resolution microCT images). The number of connections along the length of each vessel was determined, and vessels were grouped into three categories having either 0, 1 or >1 connections. For each category, number of vessels was calculated and expressed as percentage of total vessel number. This xylem network analysis was performed for the first growth ring of the stem as it represents the xylem of saplings as used for in vivo assessment of embolism formation and spread.

Percentage loss of stem hydraulic conductivity (PLC)

Based on microCT and light microscopy images of the same stem, theoretical PLC was determined from vessel number and diameter (Brodersen et al. 2013*a*). First, the volumetric flow rate of water (Q) was determined by

$$Q = \frac{\pi d^4}{128\eta}\frac{\Delta p}{\Delta x}, \quad (1)$$

(d, vessel diameter; η, viscosity of water; $\Delta p/\Delta x$ pressure gradient per length) for the total population of vessels (i.e., Q_{max}, derived from light microscopy image) and the population of embolized vessel (i.e., $Q_{embolized}$, derived from microCT images). The flow rate through the remaining functional vessels (Q_i) was determined by $Q_{max} - Q_{embolized}$. Subsequently, theoretical PLC was calculated by

$$\mathrm{PLC} = \left(1 - \frac{K_i}{K_{max}}\right) \cdot 100. \quad (2)$$

In Eq. (2), maximum hydraulic conductivity, K_{max}, was substituted by Q_{max} and hydraulic conductivity, K_i, by $Q_{embolized}$, which holds for $\Delta p/\Delta x$ = constant. For $n = 3$ plants included in Figure 2, light microscopy images were of insufficient quality to determine vessel diameters accurately, and hence K_{max} was determined from the count of total vessel number and mean vessel frequency per diameter size class shown in Figure 5.

Using the centrifuge method, PLC was measured directly on excised stem segments of 145 mm in length (Pockman et al. 1995, Choat et al. 2010). Before the stem segment was placed in the centrifuge (Sorvall RC2-B), it was degassed under house vacuum in a solution of filtered (0.2 μm) 10 mM KCl solution for

6 h to remove any embolism, and K_{max} was measured using a Sperry apparatus (e.g., Sperry et al. 2012). The stems were removed from the vacuum chamber and 3 cm of tissue was removed underwater from both ends of the sample. Subsequently, the stem segment was placed in the centrifuge rotor with both ends submerged in a water reservoir, and spun for 3 min at a velocity equal to a negative pressure gradient of $i = -0.5, -1.0, -2.0, -3.0$ and -5.0. Immediately after a spinning cycle of 3 min was completed, K_i was determined by measuring the flow rate through the sample with a pressure head of 6–8 kPa. The flow rate through the segments without the applied pressure was measured before and after each measurement, averaged and then subtracted from the K measurement to control for drift in the equilibrium values (Hacke et al. 2000, 2015). Values of K_{max} and K_i were determined by the ratio of $Q/\Delta P$, and subsequently PLC was calculated according to Eq. (2). Percentage loss of stem hydraulic conductivity was determined from $n = 10$ saplings.

Data analysis

Statistical and regression analysis were performed with SAS (version 9.2, SAS Institute, Cary, NC, USA) and SigmaPlot (version 8.0, Systat Software Inc., San Jose, CA, USA). Mean values and standard errors were determined using the 'PROC MEANS' procedure in SAS. Statistical differences were determined by analysis of variance using the 'PROC GLM' procedure in SAS.

Results

In vivo analysis of *J. microcarpa* saplings showed that under well-watered and low drought stress conditions (i.e., Ψ_{stem} from 0 to -2 MPa), xylem vessels in the stem were not susceptible to cavitation as all vessels remained water filled within this water potential range (Figures 1a and 2a). Under increasing drought stress, embolized vessels were first detected at $\Psi_{stem} < -2.2$ MPa (Figures 1b and 2a), and were located mainly in the inner two-thirds of the xylem (Figure 1b). Cavitation occurred first in isolated vessels (i.e., no air-filled conduits or obvious air spaces in close proximity) (Figure 3). Under more severe drought stress ($\Psi_{stem} < -3.3$ MPa), large numbers of embolized vessels were detected further from the pith towards the cambium (Figure 1c and d), and the pith remained largely hydrated. This apparent embolism spread is illustrated in 2- and 3-D for a representative

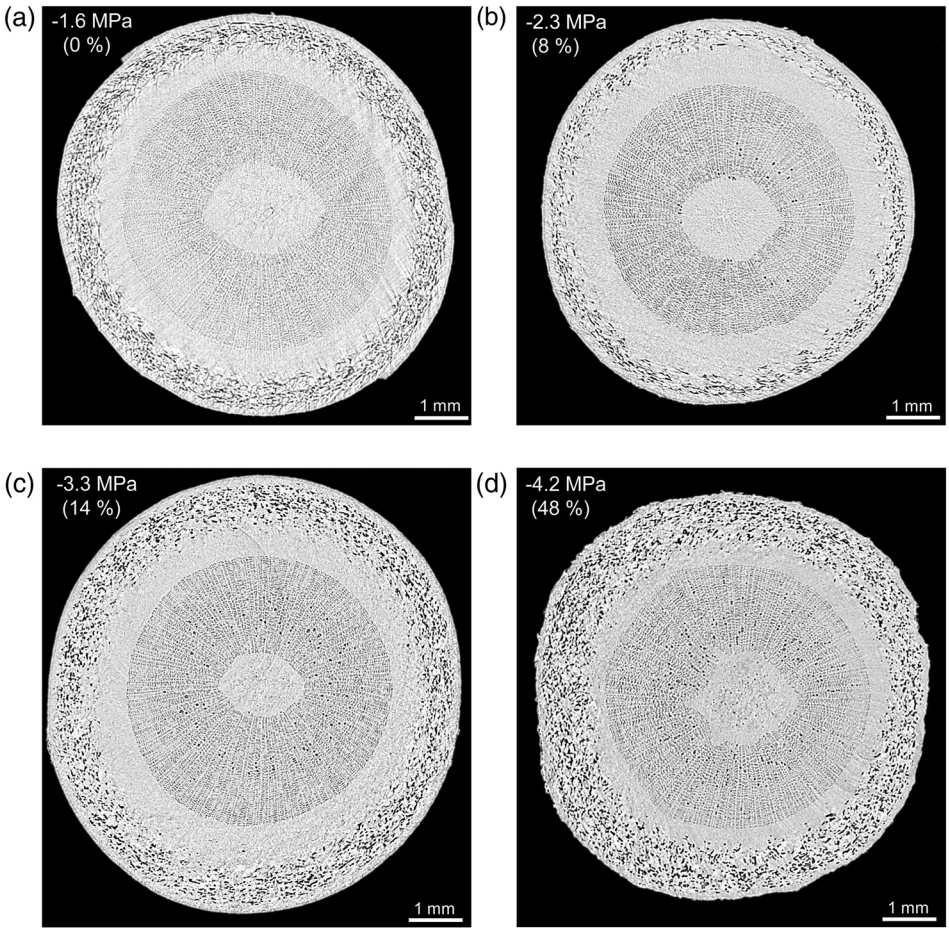

Figure 1. Representative transverse microCT images through the stem of walnut (*J. microcarpa*) saplings subjected to drought stress. Each image shows embolized vessel in dark grey and water-filled tissue in light grey. Values in each image are the stem water potential (in MPa) and corresponding amount of embolism (in % of total).

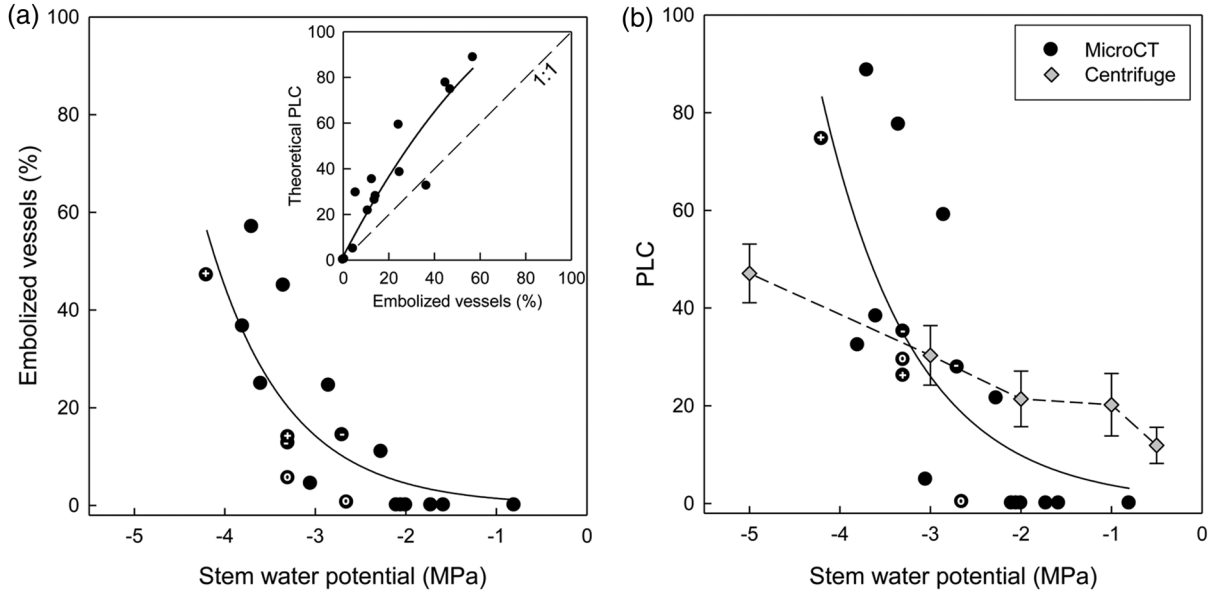

Figure 2. Xylem vulnerability in the stem of *J. microcarpa* saplings in response to drought. (a) Number of embolized vessels as percentage of total determined in vivo from microCT images (solid line is best fit, $y = 0.46e^{-1.14x}$, $R^2 = 0.68$, $P < 0.0001$); inset shows the relationship of percentage of embolized vessels and corresponding PLC as calculated from vessel diameter and number (solid line is best fit, $y = 1.67 + 1.91x - 0.01x^2$, $R^2 = 0.90$, $P < 0.0001$). (b) Percentage loss of conductivity as a function of stem water potential derived from microCT images (solid line is best fit, $y = 1.41e^{-0.97x}$, $R^2 = 0.59$, $P < 0.0001$) and measured hydraulically using the centrifuge method. An additional data point for the centrifuge method was collected at Ψ_{stem} of −7.0 MPa with a corresponding PLC of 56.6 ± 7.4 (mean ± SE), but has been omitted from the figure because it is biologically irrelevant. (a and b) Each black circle represents an individual sapling. In some cases, the same sapling was scanned twice which is indicated by same symbols (plus, minus, open circle). Each grey diamond symbol is the mean PLC ± SE as obtained from $n = 9$ saplings.

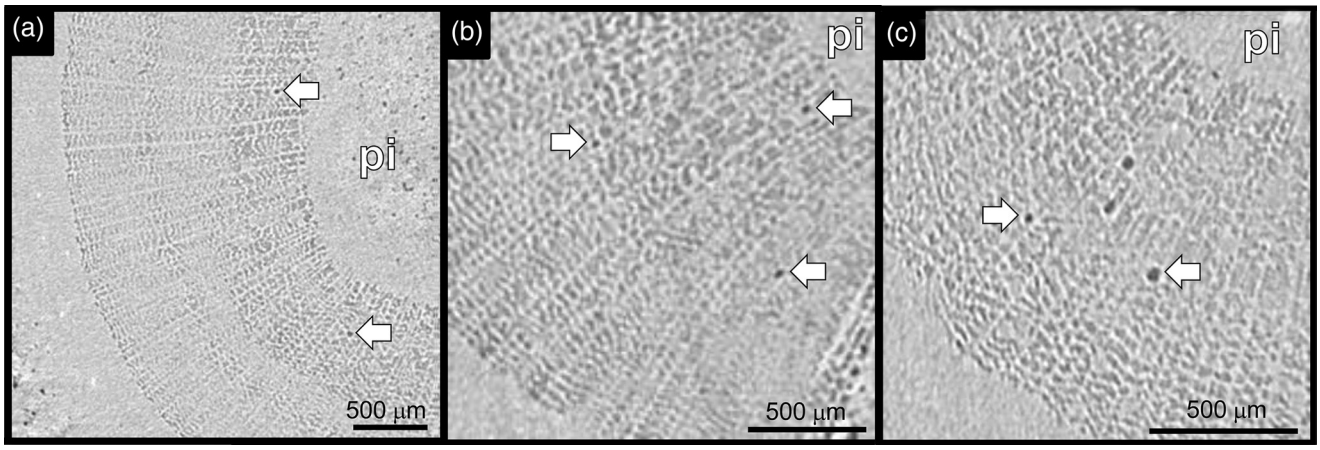

Figure 3. Representative microCT images through the stem of *J. microcarpa* showing the occurrence of isolated embolized vessels in dark grey (as also indicated by arrows) under moderate drought stress. Images were taken from $n = 3$ saplings at Ψ_{stem} of −2.7 MPa (a), Ψ_{stem} of −3.1 MPa (b) and Ψ_{stem} of −2.3 MPa (c, same sapling as in Figure 1d) (pi, pith).

sapling (Figure 4). Two-dimensional images show that groups of multiple vessels within a sector of the xylem embolized together (Figure 4a and b). Corresponding 3-D images indicated that these embolized vessels were largely separated in space but occasionally interconnected (Figure 4c–h). For example, embolized vessels 'a' and 'b' were separated in Plane 1 (Figure 4d) but came together in Plane 2 (Figure 4e), and vice versa for vessels 'c' and 'd' in the same vessel file. A direct inter-vessel connections is visualized between vessel 'c' and 'd' in Plane 1 (Figure 4d), and vessels 'e' and 'f' appeared in close proximity in Plane 1 (Figure 4g). Overall, vessels tend to run vertically with minimal contact to adjacent vessels.

The TANAX software found that in the stem of *J. microcarpa* saplings only 36% of all vessels had at least one connection to an adjacent vessel, whereas the majority of vessels (64%) lacked inter-vessel connections (Table 1; see Supplemental movie available as Supplementary Data at *Tree Physiology* Online for 3-D visualization of vessels connection). In contrast,

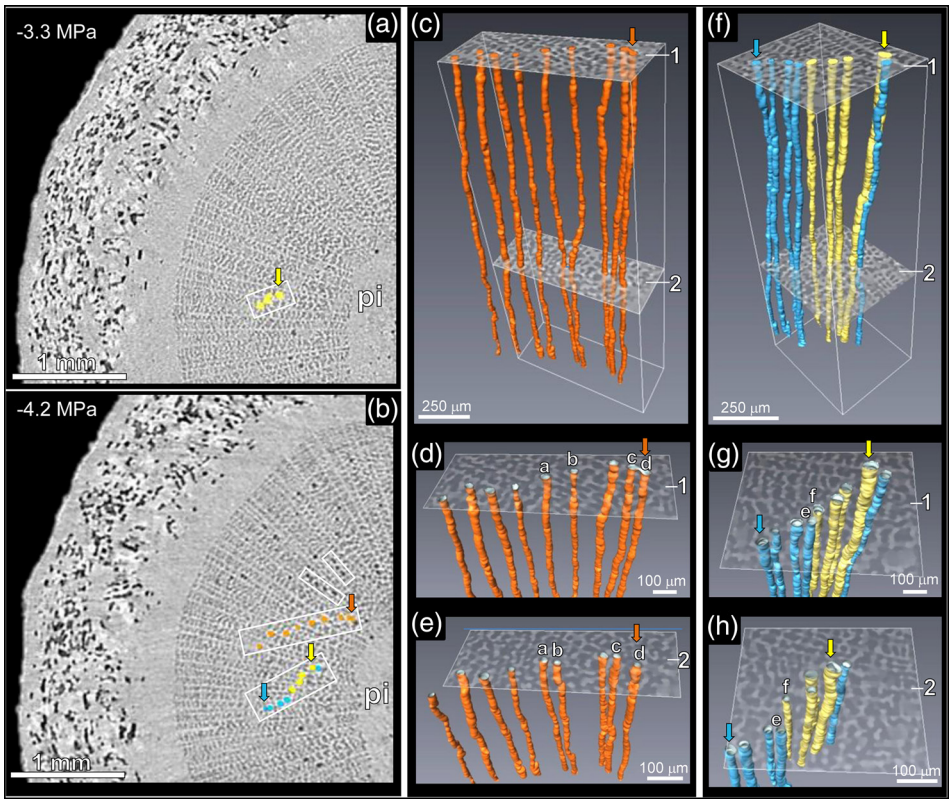

Figure 4. Visualization of embolized vessels in the stem of a *J. microcarpa* sapling subjected to increasing drought stress (same sapling as in Figures 1d and 3c). (a and b) Transverse microCT images showing radial files (indicated by white boxes) of embolized vessels at Ψ_{stem} of –3.3 MPa (a) and –4.2 MPa (b). Radial files of embolized vessels as shown in colour in (b) were reconstructed in 3-D in (c–h). Same colours (yellow, orange and blue) indicate the same vessels in (a and b) and (c–h). Same coloured arrows indicate the same individual vessel in (a and b) and (c–h). 3-D reconstructions show that embolized vessels change in proximity (i.e., compare the distance between the same two vessels [examples labelled with same small letters) in panel 1 (d and g) with panel 2 (e and h)] (pi, pith).

Table 1. Estimates of xylem network connectivity as obtained from a TANAX. A dried stem segment of *J. microcarpa* was scanned using microCT, and the percentage of vessels (n = vessel number) with 0, 1 and >1 inter-vessel pit connections was determined by TANAX software. An inter-vessel pit connection was established for a 'threshold-distance' between two adjacent vessels <12 µm (i.e., estimated thickness of double vessel wall). For comparison, TANAX data as collected on grapevine stems by Brodersen et al. (2011) are included.

	J. microcarpa (this study)	*V. vinifera* (Brodersen et al. 2011)
Analysed segment length	5.93 mm	4.5 mm
Number of vessels	$n = 378$	$n = 65$
Connections = 0	64% ($n = 242$)	24%
Connections = 1	26% ($n = 98$)	54%
Connections > 1	10% ($n = 38$)	22%

Brodersen et al. (2011) found that for *Vitis vinifera* the majority of vessels (i.e., 76%) were interconnected. In terms of xylem development of *J. microcarpa* saplings, vessels in the first year appeared to be more dispersed and generally smaller in diameter as compared with the relatively large diameter vessels that formed initially in the second year (see Figure S1 available as Supplementary Data at *Tree Physiology* Online). Saplings used in the current study for analysis of drought-induced xylem vulnerability only contained the first annual growth ring.

The percentage loss of stem hydraulic conductivity (PLC) of *J. microcarpa* saplings in response to drought stress was derived from microCT data of Figure 2a, and measured on excised stem segments with the centrifuge method (Figure 2b). Theoretical PLC values, as calculated based on vessel number and diameter, were generally higher than corresponding percentages of embolized vessels (Figure 2a, inset). The vulnerability curve generated with theoretical PLC estimates exhibited an exponential shape and indicated that 50% of conductivity was lost (PLC_{50}) at Ψ_{stem} of ~ –3.5 MPa. In contrast, using the centrifuge method PLC estimates increased rather linearly with decreasing Ψ_{stem}, and this method predicted that 20% of stem conductivity was lost already at Ψ_{stem} > –2 MPa and PLC_{50} was at Ψ_{stem} ~ –5 MPa. Ψ_{stem} in intact *J. microcarpa* saplings never approached –5 MPa as leaves were completely wilted and often scorched. The PLC estimates obtained with both methods agreed only within the Ψ_{stem} range of ~–2.5 to –3.5 MPa.

Drought-induced embolism susceptibility of xylem vessel in the stem was related to vessel diameter (Figure 5). At Ψ_{stem} of –2 to –3 MPa, larger diameter vessels of ≥40 µm embolized

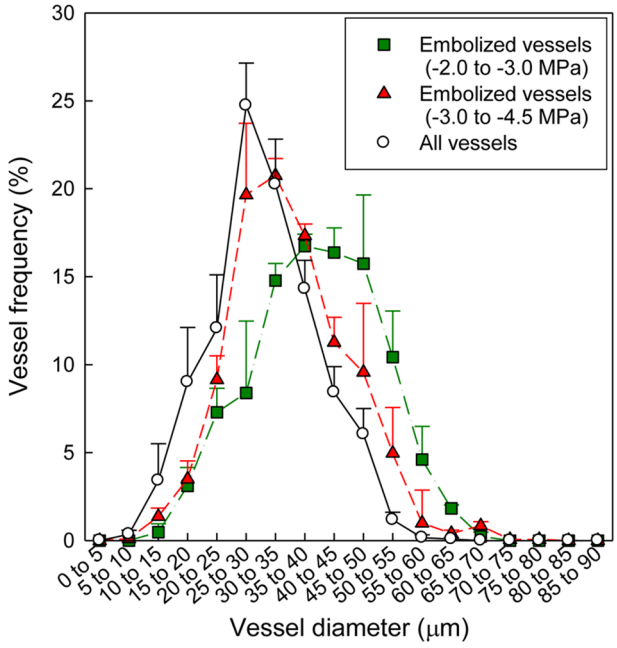

Figure 5. Vessel diameter distributions of all vessels in the stem of *J. microcarpa*, and exclusively of embolized vessels at moderate (Ψ_{stem} of −2 to −3 MPa) and severe (Ψ_{stem} of −3 to −4 MPa) drought stress. Vessel diameter distributions of all vessels and embolized vessels were generated based on light microscopy and microCT images, respectively. Each data point is the mean ± SE ($n = 9$ saplings) in vessel frequency for a given vessel diameter size class. ANOVA analysis found a significant ($P = 0.0021$) interaction between vessel diameter and drought stress (i.e., Ψ_{stem}) effect on embolized vessel frequency (dependent variable).

most frequently. Under severe drought stress (Ψ_{stem} of −3 to −4.5 MPa), there was a significant shift in the frequency of embolized vessels towards the ones of the smaller diameter of 25–40 μm (interaction term vessel diameter and Ψ_{stem}, $P < 0.01$). Vessel distributions show that vessels with a diameter of 25–30 μm were the most frequent (i.e., 25%) among all vessels in the xylem tissue. If vulnerability to cavitation was not related to vessel size, we would have predicted that more vessels in this most abundant size class (i.e., 25–30 μm) would have cavitated most frequently.

To investigate the difference in embolism susceptibility between different xylem regions, the xylem was divided into three regions, i.e., inner region close to pith, middle region and outer region towards cambium, as indicated in light micrograph of Figure 6a (see also that vessels were arranged isolated or in radial files, diffuse-porous character of xylem). Vessel distribution profiles indicated that small diameter vessels of <30 μm were most frequent in the outer xylem region, whereas larger diameter vessels of >30 μm were more frequent in the inner and middle (especially for >50 μm) xylem region (Figure 6b). Embolism susceptibility of the outer and inner xylem region was lower when compared with the middle region (interaction term xylem region and embolized vessel, $P < 0.01$) (Figure 6c). Data in Figure 6a and b point out that low embolism susceptibility was related to high frequency of small diameter vessels in the outer xylem ring and vice versa in the middle ring. Vessel density decreased by approximately twofold from inner to outer xylem region (Table 2). Total vessel numbers and vessel density decreased significantly moving from the pith towards the cambium (Table 2).

We found no evidence for refilling of embolized vessels after drought-stressed saplings were re-watered (Figure 7). MicroCT images collected on the same sapling indicated that tissue outside the xylem including phloem, cambium and bark rehydrated after 17 h, but number of embolized vessels remained similar (Figure 7a). In both representative saplings, stem water potential recovered from <−2 MPa to >−1 MPa after 15 h of re-watering, but percentage of embolized vessels changed non-significantly from 20 to 23% (#1) and from 8 to 9% (#2), even after 2 weeks of re-watering (Figure 7b).

Discussion

Using microCT, we visualized patterns of xylem embolism formation and spread in stems of walnut (*J. microcarpa*) saplings subjected to drought stress. Our data indicate that low xylem vulnerability to cavitation in the first year of growth of this species (PLC_{50} at $\Psi_{stem} \sim -3.5$ MPa) compared with others (e.g., *Juglans regia*, Tyree et al. 1993; *V. vinifera*, Brodersen et al. 2013*a*) is linked to the presence of small diameter vessels, and likely associated with low inter-vessel connectivity (compared with *V. vinifera*, Brodersen et al. 2011). Under well-watered and low drought conditions ($\Psi_{stem} > -2$ MPa), microCT images showed that all vessels in the stem were water-filled. Vessels that embolized first under drought stress ($\Psi_{stem} < -2$ MPa) were isolated (i.e., not adjacent to any air-filled vessels). Under severe drought stress ($\Psi_{stem} < -3$ MPa) multiple vessels within a sector of the xylem cavitated at the same time (i.e., embolism spread), and we speculate that this was due to air-seeding through inter-vessel connections, especially in the inner portion of the growth ring where vessel density was greatest. In line with these findings, embolism spread throughout the xylem network of grapevines was found to be associated with inter-vessel connectivity and facilitated by high xylem network connectivity (Brodersen et al. 2011, 2013*b*). In *J. microcarpa* only 36% of vessels were interconnected. Vessel diameter distribution profiles as generated from light and microCT images of *J. microcarpa* demonstrated that small diameter vessels were most abundant and were less susceptible to drought-induced cavitation than larger ones (>40 μm). Similarly, the tropical tree *Miconia argentea* was found to be more resistant to drought-induced cavitation because of high frequency of small diameter vessels (McCulloh et al. 2012). After re-watering of *J. microcarpa* saplings, there was no evidence for embolism repair in the stem similar to our previous findings on coastal redwood (Choat et al. 2015).

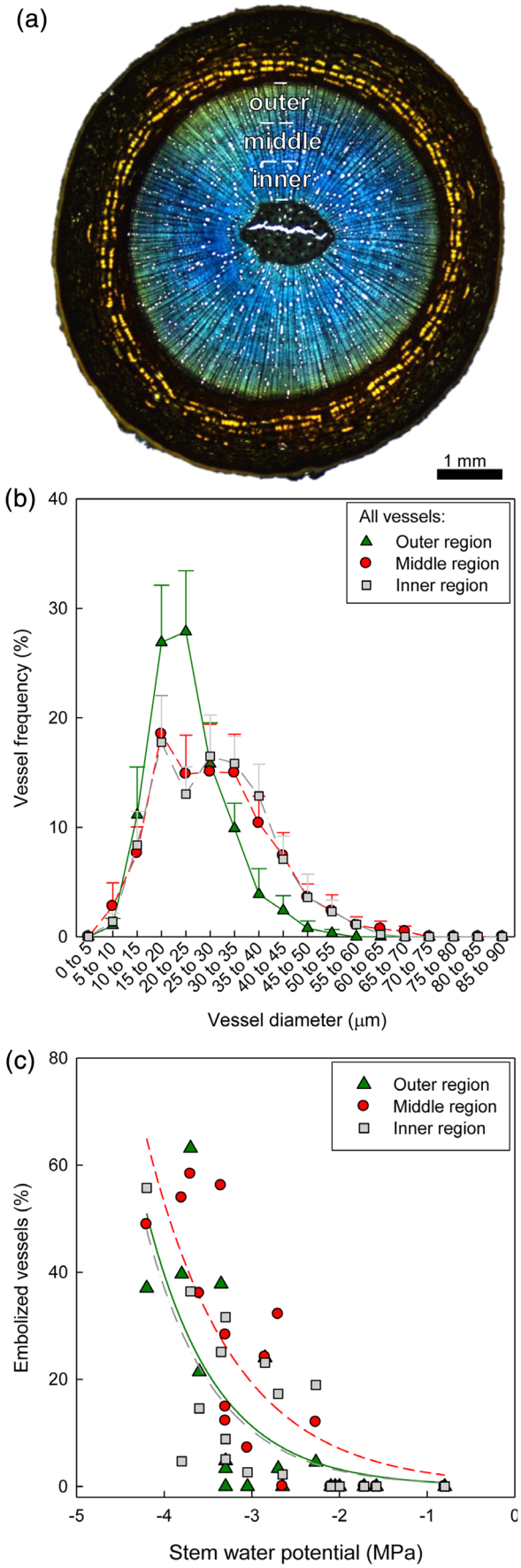

Xylem vulnerability

There is evidence in the literature that some invasive hydraulic methods tend to overestimate xylem vulnerability, especially for long-vesselled species (e.g., Choat et al. 2010, McElrone et al. 2012, Torres-Ruiz et al. 2015, Martin-StPaul et al. 2014, Wang et al. 2014, Cochard et al. 2015). In this study we used the non-invasive microCT method to determine xylem vulnerability of *J. microcarpa* saplings, which indicated no embolism formation at $\Psi_{stem} > -2$ MPa and PLC_{50} at Ψ_{stem} of ~−3.5 MPa. In comparison, PLC values obtained with the centrifuge method ranged from 10 to 21% for $\Psi_{stem} > -2$ MPa, suggesting significant embolism under well-watered and low drought stress conditions, which was not apparent in intact plants. We speculate that this overestimation was due to some air introduced into the stem xylem after cutting, and in turn an overestimation of K_i, which is inevitable when using invasive hydraulic methods even if samples are excised under water (Wheeler et al. 2013, Torres-Ruiz et al. 2015), and/or an incomplete flush of embolism out of the stem segment at high pressure and in turn an underestimation of K_{max} (Espino and Schenk 2011). Moreover, at $\Psi_{stem} < -3.5$ MPa, the centrifuge method indicated lower PLC values when compared with the microCT method. Discrepancies between the methods for high water potentials (i.e., >−2 MPa) could be related to an open vessel artefact introduced with the centrifuge method (Choat et al. 2010, Cochard et al. 2010, Martin-StPaul et al. 2014, Torres-Ruiz et al. 2014). Jacobsen and Pratt (2012) and Hacke et al. (2015) suggested that the centrifuge method accurately measures vulnerability in stem segments with open vessels, but these authors did not compare their data with in vivo analysis for intact plants. The microCT system is well suited for measuring xylem vulnerability in intact stems to provide information on xylem function under native conditions.

Stems of 1-year-old *J. microcarpa* saplings were more resistant to drought-induced xylem embolism formation (microCT PLC_{50} at Ψ_{stem} ~ −3.5 MPa) compared with *J. regia* of similar age (PLC_{50} ~ −2.3 MPa; Tyree et al. 1993). While these datasets for the two species may not be quantitatively

Figure 6. Comparison of three xylem regions in the stem of *J. microcarpa* for vessel diameter distributions and xylem vulnerability. (a) As indicated in the representative light microscopy image of the stem, the xylem tissue was divided into an inner, middle and outer region. Vessels appear in white colour. (b) Vessel diameter distributions of all vessels were generated based on light microscopy images. Each data point is the mean ± SE ($n = 9$ saplings, same saplings as included in Figure 5) in vessel frequency for a given vessel diameter size class. (c) Xylem vulnerability was determined from microCT images (including $n = 9$ additional saplings). ANOVA analysis found a significant Ψ_{stem} ($P < 0.0001$) and xylem region ($P < 0.0099$) effect on embolized vessels (dependent variable), but the interaction between Ψ_{stem} and xylem region on embolized vessels was non-significant, $P = 0.1156$). An exponential fit best described the relationship of Ψ_{stem} and % embolism (inner, $R^2 = 0.58$, $P < 0.0001$, $y = 0.23e^{-1.27x}$; middle, $R^2 = 0.68$, $P < 0.0001$, $y = 0.94e^{-1.01x}$; outer, $R^2 = 0.55$, $P < 0.0001$, $y = 0.26e^{-1.26x}$).

Table 2. Vessel number, xylem cross-sectional area and vessel density of the entire stem xylem of *J. microcarpa* and separately of the inner, middle and outer xylem regions (see Figure 6a for regions). Parameters were determined from light microscopy images. Each value is given as mean ± SE of $n = 9$ saplings (same saplings as included in Figures 5 and 6b). Different letters 'a' and 'b' indicate significant differences between xylem regions (ANOVA analysis, $P < 0.05$).

	Entire xylem region	Inner xylem region	Middle xylem region	Outer xylem region
Vessel number	559 ± 71	195 ± 17[a]	173 ± 21[a]	190 ± 40[a]
Xylem area (mm^2)	16.6 ± 2.0	3.8 ± 0.4[a]	5.5 ± 0.7[b]	7.3 ± 0.9[b]
Vessel density ($n\ mm^{-2}$)	34.5 ± 5.2	53 ± 6[a]	32 ± 5[b]	27 ± 6[b]

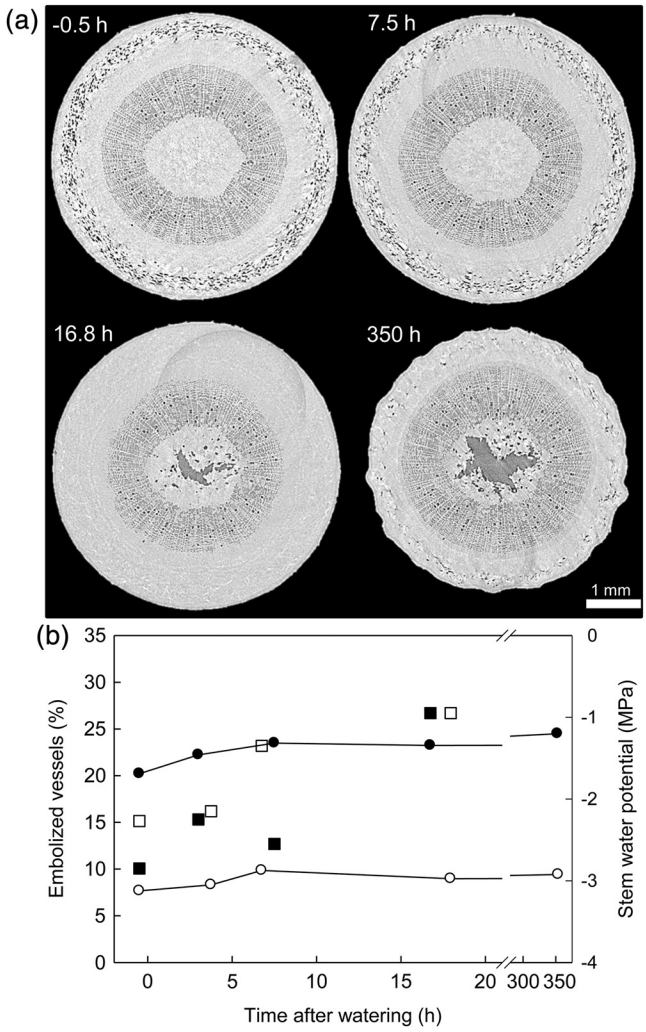

Figure 7. Refilling of embolized vessels in stems of *J. microcarpa* after re-watering. (a) Transverse microCT images of the same sapling as collected under drought stress (i.e., 30 min before re-watering) and following re-watering up to 2 weeks. Air-filled tissue and embolized vessels appear in dark grey and water-filled tissue in light grey. (b) Time course of the change in percentage of embolized vessels (circles) and stem water potential (squares) after re-watering of two saplings (#1, black symbols; #2, white symbols). MicroCT images of (a) correspond to data of #1 in (b).

comparable due to the different methods, the conclusion of greater resistant to drought-induced xylem embolism in *J. microcarpa* remains the same whether comparing them using the microCT or the centrifuge data for *J. microcarpa*. We found that low embolism susceptibility in *J. microcarpa* saplings was associated with a high abundance of small diameter vessels (25–30 μm), whereas *J. regia* is known to contain mostly large diameter vessels (100–200 μm; Schweingruber et al. 2011). In line with these findings, Davis et al. (1999) reported that species of diffuse-porous angiosperms with small diameter vessels (<30 μm, e.g., *Acer grandidentatum*) exhibited less cavitation under comparable water stress when compared with ones with larger diameter vessels (e.g., *Acer negundo*). Similar patterns have been found for other species (Hargrave et al. 1994, Sperry and Saliendra 1994, McElrone et al. 2004). Within a species, xylem in juveniles of both angiosperms and gymnosperms has been found to be more resistant to drought-induced embolism (Sperry and Saliendra 1994, Domec and Gartner 2002); such a pattern is thought to facilitate survival during establishment. Because in *J. microcarpa* xylem from the second compared with the first annual growth ring appears to have a high abundance of larger diameter vessels (see Figure S1 available as Supplementary Data at *Tree Physiology* Online), drought-induced xylem vulnerability may increase with age also in this species.

Embolism formation

Similar to coastal redwood (Choat et al. 2015), the first vessels to embolize in *J. microcarpa* were found in isolation (i.e., not attached to adjacent air-filled vessels). The occurrence of conduits that cavitate in isolation suggests that other mechanisms of nucleation besides or in addition to air-seeding across pit membranes can operate in xylem (Pickard 1981, Tyree and Sperry 1989). These mechanisms could include: (i) heterogeneous nucleation at hydrophobic cracks in vessel walls where small air bubbles can remain stable without dissolving (Pickard 1981, Tyree and Sperry 1989), (ii) homogeneous nucleation where an air bubble not attached to the vessel wall forms in response to changes in kinetic energy of water or (iii) formation of small nanobubbles promoted by the daily fluctuations in dissolved gas content due to temperature fluctuations which coalesce and form an embolism (Schenk et al. 2015). Our current results do not allow us to conclude on the predominant mechanism that operates in *J. microcarpa* as this would require additional analysis of, e.g., wall structure and property, tensions of xylem sap and changes in xylem sap composition and temperature. However, from the above mechanism,

homogeneous nucleation is the least likely given the fact that isolated vessels in *J. microcarpa* tended to occur at the least negative Ψ_{stem} (xylem tension).

Embolism spread

MicroCT images indicated that increasing drought stress induces an apparent embolism spread across groupings of multiple vessels in *J. microcarpa* saplings. Brodersen et al. (2013*a*) reported for grapevine (*V. vinifera*) that embolism consistently started forming close to the pith and spread radially towards the cambium under increasing drought stress. This distinct pattern of embolism spread was found to be associated with high xylem network connectivity via inter-vessel pit connections and xylem vessel relays (Brodersen et al. 2011, 2013*b*). Similar to grapevine and coastal redwood (Choat et al. 2015), our data suggest that the spread of embolism (once formed) in *J. microcarpa* occurs via heterogeneous nucleation by air-seeding through inter-vessel connections after the first vessel cavitated (Tyree and Sperry 1989). However, the relatively small inter-vessel connectivity as found here for stems of *J. microcarpa* as compared with grapevine (Brodersen et al. 2011; see Table 1) suggest that the spread of air through the xylem network of *J. microcarpa* is limited.

Embolism repair

Another walnut species (*J. regia*) that is susceptible to freeze-induced cavitation during the winter can restore hydraulic transport capacity in the spring through the formation of new functional xylem, by generation of root pressure associated with sap osmotic adjustments (Ameglio et al. 2002), and/or by activity of xylem parenchyma cells associated with up-regulation of aquaporin activity (Sakr et al. 2003). Our time series of microCT images shows that *J. microcarpa* saplings lack the ability to refill non-functional vessels embolized by drought even after 2 weeks of rewatering. Our study plants were grown in pots and scanned multiple times, so additional work may be required to ensure that repeated scanning is not causing damage to the tissue. However, our recent work has shown that patterns of refilling in grapevines (Knipfer et al. 2015) and lack of refilling in other species (e.g., Choat et al. 2015) are consistent regardless of whether study plants have been scanned once or multiple times. Under the assumption that the lack of refilling is not an experimental artefact, our data suggest that restoration of water transport capacity in *J. microcarpa* would depend largely on new xylem growth, at least for these young saplings.

MicroCT

As reported in the physical sciences, X-ray exposure can induce bubble nucleation in an aqueous solution by radiolysis or heating (Greenspan and Tschiegg 1967, Grogan et al. 2014). It can be argued that the energy transmitted by X-rays of the microCT system and/or increasing temperature of the stem may have promoted embolism formation in this study. However, our microCT data collected for saplings at $\Psi_{stem} > -2$ MPa showed that after the stem was subjected to a single scan all vessels remained water-filled, suggesting that X-rays did not artificially induce embolism formation. Moreover, we have scanned well-watered plants of several species multiple times and have not seen an increase in embolized conduits over time (A. J. McElrone, unpublished data). It could also be argued that the lack of refilling in *J. microcapa* saplings subjected to multiple microCT scans may be due to X-ray damage of tissue involved in refilling. There is evidence that xylem paratracheal parenchyma surrounding vessels play an important role in embolism repair by inducing water droplet growth (grapevine, Knipfer et al. 2015), and it appears that phloem tissue is involved in refilling too (laurel, olive, Trifilò et al. 2014). However, the same microCT system as used here was used to identify embolism repair in grapevine (Brodersen et al. 2010). Hence, it seems unlikely that the lack of refilling as observed here for *J. microcarpa* was mainly a result of X-ray damage. Nevertheless, future efforts must be directed in assessing the possible limitations of the microCT system for studying xylem embolism formation/repair, and we will continue to do this in all studies by combining single scan procedures (i.e., impose experimental treatments and then scan a single time) with repeated scans needed to study dynamic changes within a given plant.

Conclusion

The findings of this study on *J. microcarpa* saplings emphasize that negative effects of drought stress on xylem functionality are reduced when frequency of small diameter vessels is high. Based on a comparison of xylem network connectivity between *J. microcarpa* (as estimated here) and *V. vinifera* (Brodersen et al. 2011), we speculate that low vessel connectivity in *J. microcarpa* helps to limit embolism spread under drought stress. These xylem anatomical features most likely reflect a trade-off between providing sufficient hydraulic transport capacity and securing xylem function under drought stress. For *J. microcarpa*, our data provide evidence that xylem vulnerability to cavitation measured in vivo using microCT differs from invasive techniques like the centrifuge method. Our data emphasize that using microCT in intact plants provides a more comprehensive understanding of the dynamics embolism formation, spread and repair.

Supplementary data

Supplementary data for this article are available at *Tree Physiology* Online.

Acknowledgments

We thank D. Parkinson and A. MacDowell for their assistance at the Lawrence Berkeley National Laboratory Advanced Light

Source beamline 8.3.2 microtomography facility, and S. Castorani, A.J. Eustis and Z. Nasafi for assistance with image capture/analysis.

Conflict of interest

None declared.

Funding

This work was supported by US Department of Agriculture-Agricultural Research Service Current Research Information System funding (research project no. 5306-21220-004-00). The Advanced Light Source is supported by the Director, Office of Science, Office of Basic Energy Sciences, of the US Department of Energy (contract no. DE-AC02-05CH11231).

References

Ameglio T, Bodet C, Lacointe A, Cochard H (2002) Winter embolism, mechanisms of xylem hydraulic conductivity recovery and springtime growth patterns in walnut and peach trees. Tree Physiol 22:1211–1220.

Brodersen CR, McElrone AJ, Choat B, Matthews MA, Shackel KA (2010) The dynamics of embolism repair in xylem: in vivo visualizations using high-resolution computed tomography. Plant Physiol 154:1088–1095.

Brodersen CR, Lee EF, Choat B, Jansen S, Phillips RJ, Shackel KA, McElrone AJ, Matthews MA (2011) Automated analysis of three-dimensional xylem networks using high-resolution computed tomography. New Phytol 191:1168–1179.

Brodersen CR, McElrone AJ, Choat B, Lee EF, Shackel KA, Matthews MA (2013*a*) In vivo visualizations of drought-induced embolism spread in *Vitis vinifera*. Plant Physiol 161:1820–1829.

Brodersen CR, Choat B, Chatelet DS, Shackel KA, Matthews MA, McElrone AJ (2013*b*) Xylem vessel relays contribute to radial connectivity in grapevine stems (*Vitis vinifera* and *V. arizonica*; Vitaceae). Am J Bot 100:314–321.

Brodribb TJ, Cochard H (2009) Hydraulic failure defines the recovery and point of death in water-stressed conifers. Plant Physiol 149:575–584.

Choat B (2013) Predicting thresholds of drought-induced mortality in woody plant species. Tree Physiol 33:669–671.

Choat B, Drayton WM, Brodersen C, Matthews MA, Shackel KA, Wada H, McElrone AJ (2010) Measurement of vulnerability to water stress-induced cavitation in grapevine: a comparison of four techniques applied to a long-vesseled species. Plant Cell Environ 33:1502–1512.

Choat B, Jansen S, Brodribb TJ et al. (2012) Global convergence in the vulnerability of forests to drought. Nature 491:752–755.

Choat B, Brodersen CR, McElrone AJ (2015) Synchrotron X-ray microtomography of xylem embolism in *Sequoia sempervirens* saplings during cycles of drought and recovery. New Phytol 205:1095–1105.

Cochard H, Herbette S, Barigah T, Badel E, Ennajeh M, Vilagrosa A (2010) Does sample length influence the shape of xylem embolism vulnerability curves? A test with the cavitron spinning technique. Plant Cell Environ 33:1543–1552.

Cochard H, Badel E, Herbette S, Delzon S, Choat B, Jansen S (2013) Methods for measuring plant vulnerability to cavitation: a critical review. J Exp Bot 64:4779–4791.

Cochard H, Delzon S, Badel E (2015) X-ray microtomography (micro-CT): a reference technology for high-resolution quantification of xylem embolism in trees. Plant Cell Environ 38:201–206.

Davis SD, Sperry JS, Hacke UG (1999) The relationship between xylem conduit diameter and cavitation caused by freezing. Am J Bot 86:1367–1372.

Dixon HH, Joly J (1895) On the ascent of sap. Philos Trans R Soc Lond B Biol Sci 186:563–576.

Domec JC, Gartner BL (2002) Age- and position-related changes in hydraulic versus mechanical dysfunction of xylem: inferring the design criteria for Douglas-fir wood structure. Tree Physiol 22:91–104.

Espino S, Schenk HJ (2011) Mind the bubbles: Achieving stable measurements of maximum hydraulic conductivity through woody plant samples. J Exp Bot 62:1119–1132.

Greenspan M, Tschiegg CE (1967) Radiation-induced acoustic cavitation; apparatus and some results. J Res Natl Bur Stand 71C:299–312.

Grogan JM, Schneider NM, Ross FM, Bau HH (2014) Bubble and pattern formation in liquid induced by an electron beam. Nano Lett 14:359–364.

Hacke UG, Sperry JS, Pittermann J (2000) Drought experience and cavitation resistance in six shrubs from the great basin, Utah. Basic Appl Ecol 1:31–41.

Hacke UG, Venturas MD, MacKinnon ED, Jacobsen AL, Sperry JS, Pratt RB (2015) The standard centrifuge method accurately measures vulnerability curves of long-vesselled olive stems. New Phytol 205:116–127.

Hargrave KR, Kolb KJ, Ewers FW, Davis SD (1994) Conduit diameter and drought-induced embolism in *Salvia mellifera* Greene (Labiatae). New Phytol 126:695–705.

Jacobsen AL, Pratt RB (2012) No evidence for an open vessel effect in centrifuge-based vulnerability curves of a long-vesselled liana (*Vitis vinifera*). New Phytol 194:982–990.

Knipfer T, Eustis A, Brodersen C, Walker AM, McElrone AJ (2015) Grapevine species from varied native habitats exhibit differences in embolism formation/repair associated with leaf gas exchange and root pressure. Plant Cell Environ; doi:10.1111/pce.12497.

Martin-StPaul NK, Longepierre D, Huc R, Delzon S, Burlett R, Joffre R, Rambal S, Cochard H (2014) How reliable are methods to assess xylem vulnerability to cavitation? The issue of 'open vessel' artifact in oaks. Tree Physiol 34:894–905.

McCulloh KA, Johnson DM, Meinzer FC, Voelker SL, Lachenbruch B, Domec JC (2012) Hydraulic architecture of two species differing in wood density: opposing strategies in co-occurring tropical pioneer trees. Plant Cell Environ 35:116–125.

McElrone AJ, Pockman WT, Martinez-Vilalta J, Jackson RB (2004) Variation in xylem structure and function in stems and roots of trees to 20 m depth. New Phytol 163:507–517.

McElrone AJ, Brodersen CR, Alsina MM, Drayton WM, Matthews MA, Shackel KA, Wada H, Zufferey V, Choat B (2012) Centrifuge technique consistently overestimates vulnerability to water stress-induced cavitation in grapevines as confirmed with high-resolution computed tomography. New Phytol 196:661–665.

McElrone AJ, Choat B, Parkinson DY, MacDowell AA, Brodersen CR (2013) Using high resolution computed tomography to visualize the three dimensional structure and function of plant vasculature. J Vis Exp 74:e50162.

Pickard WF (1981) The ascent of sap in plants. Prog Biophys Mol Biol 37:181–229.

Pockman WT, Sperry JS, O'Leary JW (1995) Sustained and significant negative water pressure in xylem. Nature 378:715–716.

Rockwell FE, Wheeler JK, Holbrook NM (2014) Cavitation and its discontents: opportunities for resolving current controversies. Plant Physiol 164:1649–1660.

Rosner S (2015) A new type of vulnerability curve: is there truth in vine? Tree Physiol 35:410–414.

Sakr S, Alves G, Morillon R, Maurel K, Decourteix M, Guilliot A, Fleurat-Lessard P, Julien JL, Chrispeels MJ (2003) Plasma membrane aquaporins

are involved in winter embolism recovery in walnut tree. Plant Physiol 133:630–641.
Schenk HJ, Steppe K, Jansen S (2015) Nanobubbles: a new paradigm for air-seeding in xylem. Trends Plant Sci 20:199–205.
Schweingruber FH, Börner A, Schulze ED (2011) Atlas of stem anatomy in herbs, shrubs and trees. Volume 1. Springer, Heidelberg, Dordrecht, London, New York.
Sperry JS, Saliendra NZ (1994) Intra- and inter-plant variation in xylem cavitation in *Betula occidentalis*. Plant Cell Environ 17:1233–1241.
Sperry JS, Christman MA, Torres-Ruiz JM, Taneda H, Smith DD (2012) Vulnerability curves by centrifugation: is there an open vessel artefact, and are 'r' shaped curves necessarily invalid? Plant Cell Environ 35:601–610.
Torres-Ruiz JM, Cochard H, Mayr S, Beikircher B, Diaz-Espejo A, Rodriguez-Dominguez CM, Badel E, Fernández JE (2014) Vulnerability to cavitation in *Olea europaea* current-year shoots: further evidence of an open-vessel artifact associated with centrifuge and air-injection techniques. Physiol Plant 152:465–474.
Torres-Ruiz JM, Jansen S, Choat B et al. (2015) Direct X-ray microtomography observation confirms the induction of embolism upon xylem cutting under tension. Plant Physiol 167:40–43.
Trifilò P, Raimondo F, Lo Gullo MA, Barbera PM, Salleo S, Nardini A (2014) Relax and refill: xylem rehydration prior to hydraulic measurements favours embolism repair in stems and generates artificially low PLC values. Plant Cell Environ 37:2491–2499.
Tyree MT, Sperry JS (1989) Vulnerability of xylem to cavitation and embolism. Annu Rev Plant Physiol Plant Mol Biol 40:19–36.
Tyree MT, Zimmermann MH (2002) Xylem structure and the ascent of sap. Springer, New York.
Tyree MT, Cochard H, Cruiziat P, Sinclair B, Ameglio T (1993) Drought-induced leaf shedding in walnut: evidence for vulnerability segmentation. Plant Cell Environ 16:879–882.
Wang R, Zhang L, Zhang S, Cai J, Tyree MT (2014) Water relations of *Robinia pseudoacacia* L.: do vessels cavitate and refill diurnally or are R-shaped curves invalid in *Robinia*? Plant Cell Environ 37:2667–2678.
Wheeler JK, Huggett BA, Tofte AN, Rockwell FE, Holbrook NM (2013) Cutting xylem under tension or supersaturated with gas can generate PLC and the appearance of rapid recovery from embolism. Plant Cell Environ 36:1938–1949.
Zimmermann MH, Brown CL (1971) Trees: structure and function. Springer, Berlin.